Bulk and inhomogeneous mixtures of hard rods and excluded-volume polymer: A density functional approach

Paweł Bryk*
Department for the Modeling of Physico-Chemical Processes, Maria Curie-Skłodowska University, 20-031 Lublin, Poland

Roland Roth
Max-Planck-Institut für Metallforschung, Heisenbergstrasse 3, D-70569 Stuttgart, Germany
and Institut für Theoretische und Angewandte Physik, Universität Stuttgart, Pfaffenwaldring 57, D-70569 Stuttgart, Germany
(Received 16 September 2004; revised manuscript received 12 November 2004; published 28 January 2005)

We present a density functional theory for a mixture of hard rods and polymer modeled as chains of hard tangent spheres which refines the theory proposed in the paper by Bryk [Phys. Rev. E **68**, 062501 (2003)]. The improvement involves a semiempirical formula for the contact value of the sphere-sphere radial distribution function of the sphere and needle reference system, which includes the important depletion effect induced by the needles. The new functional yields slightly broader phase coexistence envelopes but the changes affect mainly the polymer-rich binodal branches. After analyzing the bulk phase behavior the structure of hard-rod–polymer mixture close to a hard wall is examined. An increase of the chain length leads to an increase of the average polymer segment contact value. This behavior may lead to a qualitative difference of the polymer segment profiles: from an effective repulsion of the polymer segments to an effective attraction, which can be observed by a change of sign of the excess adsorption. By analyzing the orientational order parameter profiles we have found that the polymer coils decrease the tendency of needles to adopt anisotropic configurations.

DOI: 10.1103/PhysRevE.71.011510 PACS number(s): 61.20.Gy, 64.70.Ja, 61.30.Cz

I. INTRODUCTION

Mixtures of nonadsorbing polymer and colloidal particles often exhibit a phase separation [1] even if all interactions are purely repulsive. A simple theoretical model giving an insight into this phenomenon is the Asakura-Oosawa-Vrij (AOV) model of colloid-polymer mixtures [2,3] where the ideal polymer coils (modeled as spheres) can freely overlap but the polymer-colloid and colloid-colloid interactions are hard sphere like. A tendency of the system to reduce the volume excluded to the depletion agent, in this case the polymer coils, gives rise to attractive depletion interactions between the colloidal particles. There are many experiments concerning phase transitions in bulk systems; for a recent review see, e.g., Ref. [4]. In one experiment [5] the free interface of a demixed colloid-polymer mixture was observed in real space and its thermal capillary waves were studied. Recently, studies of inhomogeneous colloid-polymer mixtures were also initiated. It has turned out that mixtures of colloids and polymer, when brought close to a hard wall, may develop a sequence of layering transitions in the partial wetting regime prior to a transition to complete wetting [6,7]. The so-called entropic wetting transition was confirmed experimentally by recent measurements of the contact angle in mixtures of silica particles and polydimethylsiloxan dispersed in cyclohexane [8,9].

Other macroparticles, such as silica coated boehmite rods or stiff polymeric rods [10–12], have been also successfully used as depletion agents in colloidal suspensions. Bolhuis and Frenkel (BF) introduced a simple model of a mixture consisting of hard sphere colloids and hard infinitely thin rods [13]. Although the vanishing thickness and volume constitutes a significant simplification (e.g., it rules out the isotropic-nematic transition), the proposed model does capture the basic features of the above-mentioned experimental systems. Bolhuis and Frenkel determined the phase diagrams of the fluid-fluid demixing transition by means of Gibbs ensemble Monte Carlo simulations and free volume theory and found a good agreement between the theory and simulations.

Among various theoretical approaches density functional theory (DFT) appears to be particularly well suited to study various problems associated with inhomogeneous fluids [14]. It has emerged that fundamental measure theory (FMT) [15] provides a very accurate description of multicomponent hard spheres. This approach is based on the deconvolution of the Mayer f functions in terms of weight functions which depend on the geometrical properties of the spheres. Rosenfeld [16] generalized his approach to mixture of convex hard-body molecules formulating thus a very general framework, based on geometrical properties of the particles, for treatment of complex, multicomponent fluids [17–19]. Although the decomposition of the corresponding Mayer f functions in terms of a finite number of convolutions of weight functions is not possible for the arbitrary hard-body fluid, Schmidt [20] was able to provide an important, specific counterexample where such deconvolution is possible. His density functional theory for mixtures of vanishingly thin hard rod and hard spheres [20] incorporates the exact low-density limit and yields the same equation of state as that of Ref. [13]. It is worth noting that Schmidt's functional gives distribution profiles that are in very good agreement with simulations for inhomogeneous sphere-needle systems [21]. Most recent refinements by Brader *et al.* [22] and by Esztermann and

*Electronic address: pawel@paco.umcs.lublin.pl

Schmidt [23] aim at including effects due to nonvanishing rod thickness. FMT for hard-body anisometric particles was also used to study wetting in the BF model [24], the depletion potentials of hard spherocylinders close to a wall [25], and to investigate model amphiphilic systems [26,27].

In a recent work [29] one of us (P.B.) proposed a functional for mixtures of vanishingly thin hard rods and polymer built of freely-jointed tangent hard spheres. The functional was constructed by combining Schmidt's functional for the BF model [20] with another FMT-class theory, the Yu and Wu functional for hard-sphere polymer [30]. In the present paper we reexamine the approximation for the contact value of the radial distribution function used in Ref. [29] and propose a simple way of improvement. The new functional is used in subsequent investigations of the structure of the hard-rod–polymer fluid close to a hard wall.

II. THEORY

A. Fundamental measure theory functional

In this work we consider a mixture of hard, vanishingly thin needles (species N) of length L and polymer (species P) represented as chains built of M tangentially bonded hard-sphere segments of diameter σ. We further assume that there are no torsional or bending potentials imposed on the polymer segments, i.e., the monomers are freely jointed and any arbitrary polymer configuration free of intermolecular and intramolecular overlap is allowed. For such polymer model the total bonding potential $V_b(\mathbf{R})$ (a sum of bonding potentials v_b between the monomers) satisfies

$$\exp[-\beta V_b(\mathbf{R})] = \prod_{i=1}^{M-1} \frac{\delta(|\mathbf{r}_{i+1} - \mathbf{r}_i| - \sigma)}{4\pi\sigma^2}, \tag{1}$$

where $\mathbf{R} \equiv (\mathbf{r}_1, \mathbf{r}_2, \ldots, \mathbf{r}_M)$ denotes a set of coordinates describing the monomer positions. The needle-needle potential is $V_{NN}=0$ for all separations and orientations, while the polymer-segment–needle potential, V_{PN}, and the pair potential between two polymer segments, V_{PP}, is infinite if a pair of objects overlap and zero otherwise. A sketch of the present model is depicted in Fig. 1. Clearly, such a model of polymer is highly simplified but it satisfies the requirement of (i) polymer having excluded volume and (ii) obeying the scaling regime for sufficiently long chains. It is also, in principle, straightforward to incorporate attractive interactions between polymer segments.

In specifying the functional we closely follow Ref. [29]. We begin by writing down the grand potential Ω of the system as a functional of local densities of polymer $\rho_P(\mathbf{R})$ and needles $\rho_N(\mathbf{r}, \boldsymbol{\omega})$

$$\begin{aligned}\Omega[\rho_P(\mathbf{R}), \rho_N(\mathbf{r}, \boldsymbol{\omega})] = F[\rho_P(\mathbf{R}), \rho_N(\mathbf{r}, \boldsymbol{\omega})] \\ + \int d\mathbf{R}\rho_P(\mathbf{R})[V_{ext}^{(P)}(\mathbf{R}) - \mu_P] \\ + \int d\mathbf{r} \int \frac{d\boldsymbol{\omega}}{4\pi}\rho_N(\mathbf{r}, \boldsymbol{\omega})[V_{ext}^{(N)}(\mathbf{r}, \boldsymbol{\omega}) - \mu_N].\end{aligned} \tag{2}$$

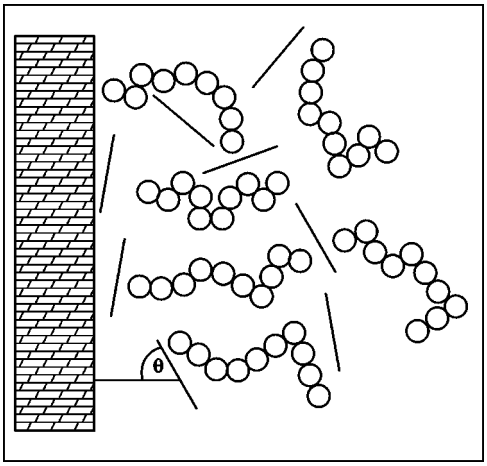

FIG. 1. Sketch of the system considered in this work. Shown are 10-mers built of freely-jointed tangent hard spheres and hard rods against a hard wall. Due to the symmetry of the problem the configuration of a needle is fully described by specifying z the distance of the center of the needle from the wall and θ the angle between the needle and the wall.

In the above $\boldsymbol{\omega}$ is a unit vector describing the orientation of the rod, $V_{ext}^{(P)}(\mathbf{R})$, μ_P, $V_{ext}^{(N)}(\mathbf{r}, \boldsymbol{\omega})$ and μ_N are the external and the chemical potentials for polymer and rods, respectively. Traditionally, the free energy of the system F is split into ideal and excess parts, $F=F_{id}+F_{ex}$. For the (exact) ideal part of the free energy we refer the reader to our earlier paper [29].

A starting point of every FMT-class DFT is the ansatz that the excess free energy density Φ can be expressed as a simple *function* of the weighted densities $n_\alpha^{(i)}$. Our prescription for Φ closely follows the first order thermodynamic perturbation theory (TPT1) of Wertheim [31], who showed that the excess free energy of a polymer system can be treated as a sum of the excess free energy of the reference system containing unbonded monomers plus a perturbation based on connecting the monomers together to form the polymer coils. What makes TPT1 extremely attractive from the practical point of view is that the perturbation excess free energy contains information about the radial distribution function (RDF) of the unbonded monomers in the reference system only.

Yu and Wu [30] extended Wertheim's first-order perturbation theory to inhomogeneous mixtures of tangentially jointed hard-sphere chains by proposing a density functional theory, where the contribution to the excess free energy density Φ_P due to the chain connectivity is expressed in terms of FMT-style weighted densities. Following Ref. [30] we assume that F_{ex} is a functional of the local density of rods and average segment densities $\rho_{PS}(\mathbf{r})$ defined as

$$\rho_{PS}(\mathbf{r}) = \sum_{i=1}^{M} \rho_{PS,i}(\mathbf{r}) = \sum_{i=1}^{M} \int d\mathbf{R}\delta(\mathbf{r} - \mathbf{r}_i)\rho_P(\mathbf{R}), \tag{3}$$

where $\rho_{PS,i}(\mathbf{r})$ is the local density of the polymer segment i. The total excess free energy of an inhomogeneous mixture of

hard rods and tangent hard-sphere chains can therefore be written as

$$\beta F_{ex} = \int d\mathbf{r} \int \frac{d\boldsymbol{\omega}}{4\pi} [\Phi_{PN}(\{n_\alpha^{(i)}\}) + \Phi_{HS}(\{n_\alpha^{(P)}\}) + \Phi_P(\{n_\alpha^{(i)}\})]. \tag{4}$$

In the above, $\Phi_{PN}+\Phi_{HS}$ describes the reference mixture of hard spheres and hard rods, while the excess free energy density due to the chain connectivity Φ_P is an "inhomogeneous counterpart" of the perturbation term in TPT1.

There are several expressions for the hard-sphere part Φ_{HS} of the excess free energy density and we have some freedom in selecting a particular formula. For the present problem we choose the "White-Bear" version of FMT [32,33] in conjunction with a modification allowing for the occurrence of a stable freezing transition [34]:

$$\Phi_{HS}(\{n_\alpha^{(P)}\}) = -n_0^{(P)} \ln(1-n_3^{(P)}) + \frac{n_1^{(P)} n_2^{(P)} - \boldsymbol{n}_{V1}^{(P)} \cdot \boldsymbol{n}_{V2}^{(P)}}{1-n_3^{(P)}} + (n_2^{(P)})^3 (1-\xi^2)^3 \frac{n_3^{(P)} + (1-n_3^{(P)})^2 \ln(1-n_3^{(P)})}{36\pi (n_3^{(P)})^2 (1-n_3^{(P)})^2}, \tag{5}$$

where $\xi(\mathbf{r}) = |\boldsymbol{n}_{V2}^{(P)}(\mathbf{r})| / n_2^{(P)}(\mathbf{r})$. The polymer weighted densities $n_\alpha^{(P)}(\mathbf{r})$ are evaluated from

$$n_\alpha^{(P)}(\mathbf{r}) = \int d\mathbf{r}' \rho_{PS}(\mathbf{r}') w_\alpha^{(P)}(\mathbf{r}-\mathbf{r}'), \tag{6}$$

where the weight functions $w_\alpha^{(P)}(\mathbf{r})$, $\alpha = 3,2,1,0,V2,V1$ are given in Ref. [20,22] and [29].

The polymer-needle contribution is taken from Schmidt's functional for hard-rod–hard-sphere mixtures [20]. Following this approach the excess free energy density due to vanishingly thin needles can be written as

$$\Phi_{PN}(\{n_\alpha^{(i)}\}) = -n_0^{(N)} \ln(1-n_3^{(P)}) + \frac{n_1^{(N)} n_2^{(PN)}}{1-n_3^{(P)}}, \tag{7}$$

where the needle weighted densities, $n_\alpha^{(N)}$, are obtained through (spatial) convolutions of the needle local density and the corresponding orientation-dependent weight functions

$$n_\alpha^{(N)}(\mathbf{r},\boldsymbol{\omega}) = \int d\mathbf{r}' \rho_N(\mathbf{r}',\boldsymbol{\omega}) w_\alpha^{(N)}(\mathbf{r}-\mathbf{r}',\boldsymbol{\omega}), \quad \alpha = 0,1. \tag{8}$$

The "mixed" polymer segment-needle weighted density, $n_2^{(PN)}$, is obtained via spatial convolution of the polymer segment density and an orientation-dependent weight function

$$n_2^{(PN)}(\mathbf{r},\boldsymbol{\omega}) = \int d\mathbf{r}' \rho_{PS}(\mathbf{r}') w_2^{(PN)}(\mathbf{r}-\mathbf{r}',\boldsymbol{\omega}). \tag{9}$$

As in every FMT, weight functions are connected with the geometrical properties of the particles. For the BF model of hard-rod–hard-sphere mixtures Schmidt was able to provide a set of $w_\alpha^{(i)}$ that leads to a *complete* deconvolution of the corresponding Mayer bond $f_{ij} = \exp(-\beta V_{ij}) - 1$. These weight functions are given in Ref. [20]. Equations (5) and (7) specify the reference part of the excess free energy.

Yu and Wu [30] proposed a way of adopting the perturbation part, based on Wertheim's TPT1, to inhomogeneous mixtures of chains of freely-jointed tangent hard spheres. For the present system we apply a similar strategy and write the excess free energy density due to the chain connectivity as

$$\Phi_P(\{n_\alpha^{(i)}\}) = \frac{1-M}{M} n_0^{(P)} \zeta \ln[y_{hs+hr}(\sigma^+;\{n_\alpha^{(i)}\})], \tag{10}$$

where $\zeta = 1 - \boldsymbol{n}_{V2}^{(P)} \cdot \boldsymbol{n}_{V2}^{(P)} / (n_2^{(P)})^2$, while y_{hs+hr} denotes the contact value of a sphere-sphere RDF in the reference mixture of hard spheres and hard rods. Unfortunately, to the best of our knowledge, no closed and accurate expression for this exists; therefore further approximations are necessary. The first guess is to ignore the influence of the rods on the contact value of the RDF completely and to approximate y_{hs+hr} by the contact value of a sphere-sphere RDF in the reference system of pure hard spheres, y_{hs}, as proposed by one of us (P.B.) in Ref. [29]. To this end we follow Ref. [30] and employ

$$y_{hs}(\sigma^+;\{n_\alpha^{(P)}\}) = \frac{1}{1-n_3^{(P)}} + \frac{n_2^{(P)} \sigma \zeta}{4(1-n_3^{(P)})^2} + \frac{(n_2^{(P)})^2 \sigma^2 \zeta}{72(1-n_3^{(P)})^3}. \tag{11}$$

It is interesting to point out that it would also be possible to follow the different approach of Ref. [35] to obtain an approximation for the contact value of the RDF. The resulting expression is slightly more complicated than Eq. (11) but yields numerically very similar results in the whole fluid range. The above equation, together with Eqs. (5), (7), and (10), completely specifies the functional, and we abbreviate this theory as DFT1. This approximation renders Φ_P independent on the density of rods.

B. Approximation for the contact value of the radial distribution function

It is expected that for high densities of rods DFT1 will lead to discrepancies connected with rod-induced depletion interactions. The overall effect is that the contact value of a sphere-sphere RDF in the hard-rod–hard-sphere mixture is higher compared to the corresponding contact value for the one-component hard-sphere fluid, $y_{hs+hr} > y_{hs}$. In order to improve the functional these depletion interactions, which in the case of noninteracting rods are found to be purely attractive, should be taken into account. We can do so by "integrating out" the needle degrees of freedom to arrive at an effective one-component description whereby colloidal spheres interact via an effective pair potential—the depletion potential $W(r)$. This approach has already been used in recent studies of depletion potentials [36] and wetting [24] in hard-rod–hard-sphere mixtures. From $W(r)$ we can extract the contact value of the sphere-sphere RDF. In principle, this can be achieved by several methods, e.g., by solving numerically the Ornstein-Zernike equation with an adequate closure or by minimizing a DFT that employs the depletion potential [24], but since we want to use this result in subsequent DFT

calculations, an analytical formula would seem more practical. Therefore, we use the well-known high temperature approximation

$$y_{hs+hr}(\sigma^+;\{n_\alpha^{(i)}\}) = y_{hs}(\sigma^+;\{n_\alpha^{(P)}\})\exp[-\beta W(\sigma^+;\{n_\alpha^{(i)}\})]. \tag{12}$$

Yaman *et al.* [37] proposed a quasiexact fit for the contact value of a depletion potential between two identical spheres (of diameter σ) immersed in a sea of hard rods of length L. For the present problem we recast it using FMT-style weighted densities

$$\beta W(\sigma^+;\{n_\alpha^{(i)}\}) = \overline{W}(\sigma,L)\frac{n_0^{(N)}}{1-n_3^{(P)}}\exp\left(\frac{L}{4}\frac{n_2^{(PN)}}{1-n_3^{(P)}}\right), \tag{13}$$

where

$$\overline{W}(\sigma,L) = -\frac{\pi}{12}L^2\sigma\frac{1+1.7524(L/\sigma)}{1+2.66396(L/\sigma)+3.929(L/\sigma)^2}. \tag{14}$$

In the limit of vanishing rod density the contact value of y_{hs+hr}, given in Eq. (12), reduces to the accurate approximation of the contact value of the RDF of a pure hard-sphere fluid, Eq. (11), and is quasiexact in the limit of vanishing sphere density. If both the sphere and the rod density is nonvanishing, the approximation of Eq. (12) can be tested numerically, e.g., by DFT within an effective one-component picture [24]. We find that, for moderate densities of the rods and sphere, Eq. (12) and the numerical results agree very nicely within a few percent. For high densities of rods and sphere the competition between packing effects and the highly attractive depletion potential reduces the contact value of the RDF considerably as compared to the high temperature approximation. However, this does not seem to be a serious problem. In the case of $M=1$, when the fluid-fluid phase separation is located at high reservoir densities of the rods and hence the discrepancy between Eq. (12) and the *real* contact value of the RDF is expected to be largest, the difference between the binodal predicted by the new and the old approach vanishes. As M is increased, the binodal of the fluid-fluid phase separation moves to lower reservoir densities of the rods and the approximation of Eq. (12) becomes more reliable. Note, however, that if the size ratio q becomes large, effective many-body interactions becomes more important so it should be expected that the predictions of the contact value of the RDF based solely on the knowledge of the depletion *pair* interaction $W(r)$ becomes less reliable.

Equations (12)–(14) together with Eqs. (5), (7), and (10) form a complete prescription for the new functional. The DFT2 theory still reduces to Schmidt's functional [20] if $M=1$ and to Yu and Wu's functional [30] if the density of rods $\rho_N=0$. The functional is *linear* in the local density of rods.

III. RESULTS

A. Demixing in the bulk phases

If the local densities of both species are isotropic, Eqs. (6), (8), and (9) can be evaluated analytically. The vector weighted densities vanish whereas the scalar weighted densities become proportional to the corresponding bulk densities. It is straightforward to obtain the corresponding expressions for the free energy, pressure, and chemical potentials of both species [29].

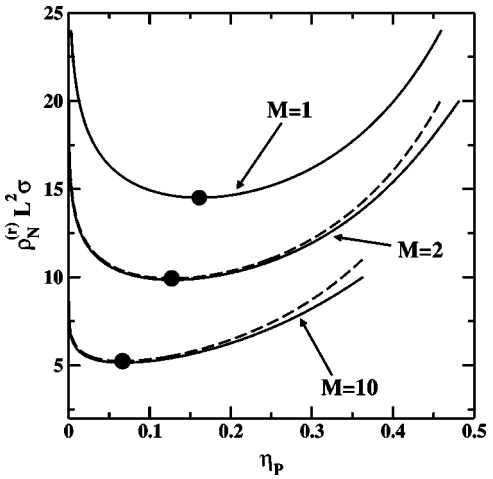

FIG. 2. Phase equilibria for hard-rod–polymer mixtures resulting from the present theory (DFT2, solid lines) and the theory from Ref. [29] (DFT1, dashed lines) plotted in the polymer packing fraction $\eta_P=(\pi/6)\sigma^3 M\rho_P$ and dimensionless needle reservoir density $\rho_N^{(r)}L^2\sigma$ representation. The binodals were evaluated for systems with size ratio $q=L/\sigma=1$ and polymer with $M=1$, 2, and 10. For $M=1$ both theories yield identical phase diagrams. Black circles indicate the critical points of the demixing transitions.

Under favorable conditions a mixture of polymer and hard rods demixes into polymer-rich (rod-poor) and polymer-poor (rod-rich) phases. The coexisting equilibrium densities (binodals), the spinodals, and the critical points were obtained by applying a procedure described in detail in Ref. [29].

In Fig. 2 we show examples of binodals resulting from the present theory DFT2 (solid lines), and from the DFT1 theory from Ref. [29] (dashed lines). The phase diagrams, plotted in the polymer packing fraction, $\eta_P=(\pi/6)\sigma^3 M\rho_P$, versus the dimensionless needle reservoir density, $\rho_N^{(r)}L^2\sigma$, representation, were evaluated for systems with $M=1,2,10$ for constant $q=L/\sigma=1$. For the special case $M=1$ (the uppermost diagram) both theories reduce to the BF theory.

We observe that, with increase of the chain length, both theories predict broadening of the phase coexistence and a shift of the critical point towards lower polymer packing fractions and lower reservoir needle densities. The binodals from DFT2 theory are somewhat broadened, especially the polymer-rich side of the diagrams, leading thus to a larger difference between the coexisting polymer densities but the overall effect is rather moderate. This may come as a surprise at first but is in fact just a fortunate consequence of the above-mentioned shift towards lower reservoir needle densities.

We have also analyzed the phase behavior in the limit of very long polymer chains resulting from DFT2 theory. Although the relevant figure is not shown here, we have verified that in the limit $M\to\infty$ the polymer critical packing fraction tends to zero. On the other hand, the rod critical

density tends to a constant virtually independent on the size ratio q. This behavior is characteristic of the so-called "protein limit" of colloid-polymer mixtures [28,38] and was also found to hold within DFT1 theory [29].

B. Hard-rod–polymer mixtures close to a hard wall

The most important feature of every DFT is the ability to describe inhomogeneous systems. In the present section we apply the theory outlined in Sec. II to describe a mixture of hard rods and tangent hard sphere chains close to a hard structureless wall. The equilibrium profiles of both species can be obtained by considering the condition

$$\frac{\delta\Omega[\rho_P(\mathbf{R}),\rho_N(\mathbf{r},\boldsymbol{\omega})]}{\delta\rho_P(\mathbf{R})}=\frac{\delta\Omega[\rho_P(\mathbf{R}),\rho_N(\mathbf{r},\boldsymbol{\omega})]}{\delta\rho_N(\mathbf{r},\boldsymbol{\omega})}=0, \quad (15)$$

which leads to the following equation for the average segment density profile

$$\rho_{PS}(\mathbf{r})=\exp(\beta\mu_P)\int d\mathbf{R}\sum_{j=1}^{M}\delta(\mathbf{r}-\mathbf{r}_j) \times\exp\left[-\beta V_b(\mathbf{R})-\beta\sum_{l=1}^{M}\lambda_l(\mathbf{r}_l)\right], \quad (16)$$

where $\lambda_j(\mathbf{r}_j)$ is given by

$$\lambda_j(\mathbf{r}_j)=\frac{\delta F_{ex}}{\delta\rho_s(\mathbf{r}_j)}+v_j(\mathbf{r}_j), \quad (17)$$

and $v_j(\mathbf{r}_j)$ being an external potential acting on the jth segment. Equation (16) can be rewritten in a more compact form

$$\rho_{PS}(\mathbf{r})=\exp(\beta\mu_P)\sum_{j=1}^{M}\exp[-\beta\lambda_j(\mathbf{r})]G_j(\mathbf{r})G_{M+1-j}(\mathbf{r}), \quad (18)$$

where the propagator function $G_j(\mathbf{r})$ is determined from the recurrence relation

$$G_j(\mathbf{r})=\int d\mathbf{r}'\exp[-\beta\lambda_j(\mathbf{r}')]\frac{\delta(\sigma-|\mathbf{r}-\mathbf{r}'|)}{4\pi\sigma^2}G_{j-1}(\mathbf{r}') \quad (19)$$

for $j=2,3,\ldots,M$ and with $G_1(\mathbf{r})\equiv 1$. Conversely, the orientation-dependent needle density profile can be obtained from

$$\rho_N(\mathbf{r},\boldsymbol{\omega})=\exp(\beta\mu_N)\exp\left[-\beta V_{ext}^{(N)}(\mathbf{r},\boldsymbol{\omega})-\beta\frac{\delta F_{ex}}{\delta\rho_N(\mathbf{r},\boldsymbol{\omega})}\right]. \quad (20)$$

In the planar symmetry the average segment density profile becomes a function of the distance z from the wall, $\rho_{PS}(\mathbf{r})\equiv\rho_{PS}(z)$, whereas the needle density profile depends on z and the orientation θ, $\rho_N(\mathbf{r},\boldsymbol{\omega})\equiv\rho_N(z,\theta)$, with $0\leqslant\theta\leqslant\pi/2$ (cf. Fig. 1). Equations (18) and (20) can be solved numerically by a standard Picard method [22,30].

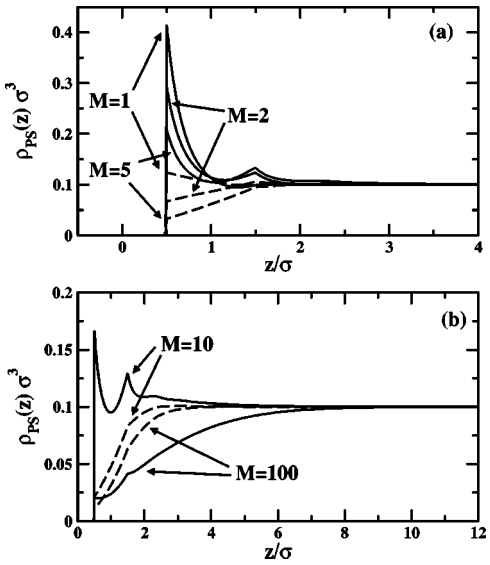

FIG. 3. Average segment density profiles of tangent hard-sphere chains with the bulk segment density $\rho_{PS}^{(b)}\sigma^3=0.1$ in a hard-rod–polymer mixture (solid lines) and in a one component system (dashed lines) close to a hard wall. The dimensionless needle (system) density $\rho_N^{(b)}L^2\sigma=4$ for all chain lengths except for $M=100$, where $\rho_N^{(b)}L^2\sigma=2.5$. The chain lengths M are marked in the figure. The size ratio in both parts $q=1$.

Let us now discuss the structure of the hard-rod polymer mixtures close to a hard wall. We restrict ourselves to the case of supercritical state points such that the system is free of the onset of the wetting transition. In Fig. 3 we show the representative examples of the average segment density profiles of tangent hard-sphere chains consisting of $M=1$, 2, 5, 10, and 100 number of beads, evaluated for the bulk segment density $\rho_{PS}^{(b)}\sigma^3=0.1$ in a hard-rod–polymer mixture (solid lines) and in a one component system (dashed lines). Bulk density of rods $\rho_N^{(b)}L^2\sigma=4$ in the system for all chain lengths except for $M=100$ in which $\rho_N^{(b)}L^2\sigma=2.5$. For systems without needles one observes that the polymer is depleted from the region close to the wall. The contact density for $M>1$ is lower than the density in the bulk. This effect, characteristic for low segment densities, has been already reported in the literature [39–41]. The addition of the needles causes the contact density to increase and the region in the vicinity of the wall is now enriched in polymer. The excess adsorption isotherm, $\Gamma=\int dz[\rho_{PS}(z)-\rho_{PS}^{(b)}]$, where we integrate from $z=\sigma/2$ where the density profile make the jump to infinity, may even change the sign; for instance, for $M=10$ [cf. Fig. 3(b)] one has $\Gamma\sigma^2=-0.055480$ for the one-component system (dashed line), whereas in the mixture (solid line) $\Gamma\sigma^2=0.034673$. Only for the longest chains studied, $M=100$ [cf. Fig. 3(b)] the lower needle density was insufficient to significantly alter the structure of the polymer fluid. In this case one observes a further broadening of the depletion zone.

Within our theory it is possible to track down the profiles of particular segments. In Fig. 4 we display the middle (solid lines) and end (dashed lines) segment density profiles for a

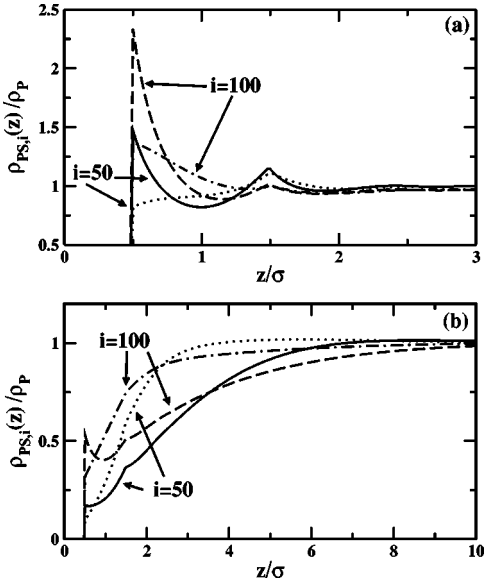

FIG. 4. Middle (solid and dotted lines) and end (dashed and dash-dotted lines) segment density profiles of tangent hard-sphere 100-mers in a hard-rod–polymer mixture (size ratio $q=1$, solid and dashed lines) and in a one component system (dotted and dash-dotted lines) close to a hard wall. The profiles in (a) were evaluated for $\rho_{PS}^{(b)}\sigma^3=0.4$ whereas in (b) for $\rho_{PS}^{(b)}\sigma^3=0.1$. The bulk needle (system) density in both parts $\rho_N^{(b)}L^2\sigma=2.5$. The profiles are normalized by the corresponding bulk density.

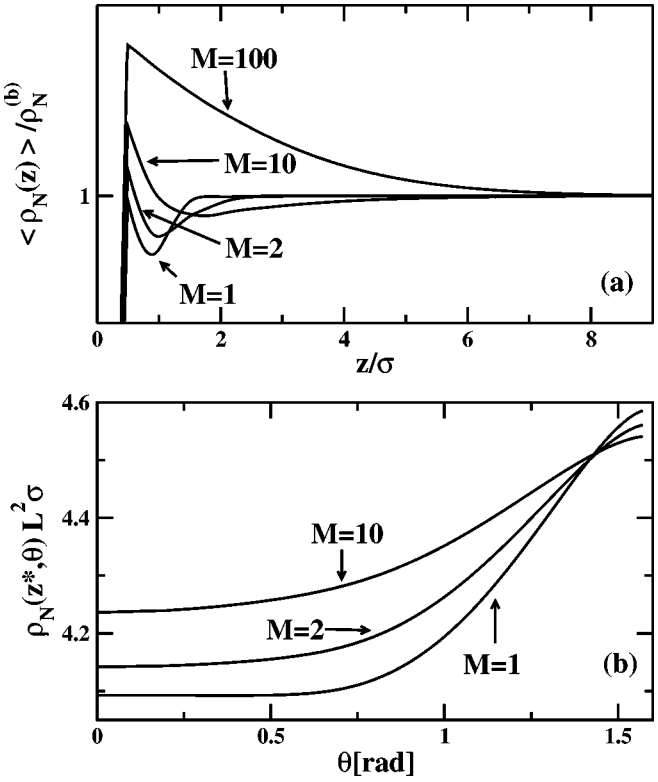

FIG. 5. (a) Orientation averaged density profiles of needles in a hard-rod–polymer mixture close to a hard wall. The profiles were evaluated for different chain lengths M listed in the figure and for the size ratio $q=1$. The bulk polymer segment density $\rho_{PS}^{(b)}\sigma^3=0.1$ whereas the bulk needle (system) density $\rho_N^{(b)}L^2\sigma=4$ for $M=1$, 2, and 10, and $\rho_N^{(b)}L^2\sigma=2.5$ for $M=100$. The profiles are normalized by the corresponding bulk density. (b) Needle density profiles evaluated along the line of closest contact with the wall $z^*(\theta)=\cos(\theta)L/2$. The profiles were evaluated for the systems corresponding to (a). The chain lengths M are marked in the figure.

mixture of hard rods and 100-mers evaluated at $\rho_{PS}^{(b)}\sigma^3=0.4$ [part (a)] and $\rho_{PS}^{(b)}\sigma^3=0.1$ [part (b)]. Shown are also the middle (dotted lines) and end (dash-dotted) segment density profiles of the cone component 100-mer fluid at the same bulk segment densities. We note that, similar to the average segment profiles from Fig. 3, the contact values of both middle and end segment profiles increased but qualitatively the structure of the profiles remains unchanged, i.e., the end segments always adsorb preferentially to the middle segments, irrespective of the polymer density. Thus we conclude that the addition of the needles does not alter qualitatively the orientation of the polymer close to the wall.

The structure of the hard rods close to the hard wall is investigated in Fig. 5. Part (a) shows the orientation averaged density profiles of needles in a mixture with polymer of different chain length. The polymer segment density $\rho_{PS}^{(b)}=0.1$, whereas the needle (system) density $\rho_N^{(b)}L^2\sigma=4$ for $M=1$, 2, and 10, and $\rho_N^{(b)}L^2\sigma=2.5$ for $M=100$. We note that for $M=1$ (i.e., for the hard-rod–hard-sphere mixture) the first sharp maximum at $z/\sigma\approx 0.5$ is slightly below the bulk needle density and is followed by a subsequent minimum. For longer chain length this minimum becomes shallower but longer ranged. This is accompanied by the gradual increase of the first maximum. Part (b) displays the orientation needle density at the distance of closest approach of the needle's center to the wall $z^*(\theta)=\cos(\theta)L/2$ for systems from Fig. 5(a). An increase of the chain length leads to an increase of the contact value for small angles and a decrease of the contact values close to $\pi/2$. This implies that an orientational order of needles at the contact decreases as the chain length increases. The integrals of the profiles from Fig. 5(b) are related to the pressure [42]. For the present case of a mixture of hard rods and polymer it can be shown that

$$\beta P = \rho_{PS}(\sigma/2) + \int \frac{d\boldsymbol{\omega}}{4\pi}\rho_N(z^*,\theta). \tag{21}$$

The present DFT is constructed so that this sum rule is satisfied and hence can be used to establish the correct implementation of the DFT and verify the numerical accuracy of our calculations. For example, for $M=10$ systems from Fig. 5 the pressure $\beta P\sigma^3=4.5475$, whereas the right-hand side of Eq. (21) obtained from numerical calculations is 4.5461 (the level of agreement depends of course on the grid size). The wall contact distribution sum rule for a model hard-body amphiphiles within FMT, which is somewhat similar to the sum rule Eq. (21), was studied in Ref. [27] and was used to verify their numerical procedures.

Further insight into the structure of the needles close to a hard wall can be inferred from the orientational order parameter profile

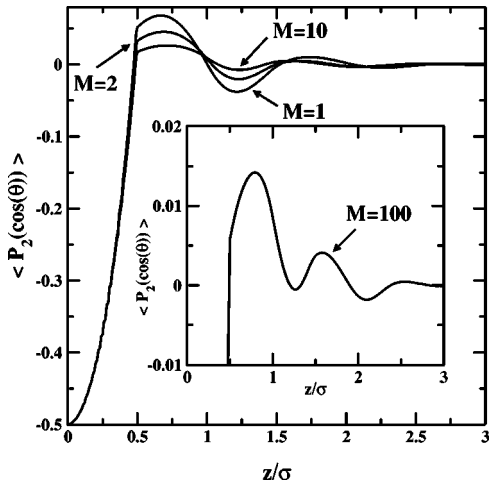

FIG. 6. Orientational order parameter profiles for a hard-rod–polymer mixture close to a hard wall. The bulk polymer segment density $\rho_{PS}^{(b)}\sigma^3=0.4$, whereas the bulk needle (system) density $\rho_N^{(b)}L^2\sigma=4$ for $M=1$, 2, and 10, and $\rho_N^{(b)}L^2\sigma=2.5$ for $M=100$. Positive values of $\langle P_2[\cos(\theta)]\rangle$ indicate normal while negative values indicate parallel orientation to the wall.

$$\langle P_2(\cos\theta)\rangle = \frac{\int d\boldsymbol{\omega}\rho_N(\mathbf{r},\boldsymbol{\omega})P_2(\cos\theta)}{\int d\boldsymbol{\omega}\rho_N(\mathbf{r},\boldsymbol{\omega})}, \qquad (22)$$

where $P_2(x)=3/2x^2-1/2$ is the second Legendre polynomial. Positive values of the order parameter indicate a tendency to align perpendicular to the wall while negative values point to parallel orientation to the wall. The order parameter profiles shown in Fig. 6 were evaluated for the systems with the polymer segment bulk density $\rho_{PS}^{(b)}=0.4$ and for the bulk needle (system) density $\rho_N^{(b)}L^2\sigma=4$ for $M=1$, 2, and 10, and $\rho_N^{(b)}L^2\sigma=2.5$ for $M=100$. The profiles show oscillations indicating that there exist mutually interleaved "layers" of needles that prefer normal and parallel orientation. As the distance from the wall increases, these oscillations are gradually damped. An increase of the chain length leads to a stronger dampening effect and decreases the tendency of needles to adopt anisotropic configurations.

IV. CONCLUSIONS

In this work we propose an improved version of the fundamental measure theory for mixtures of hard rods and polymer built of freely-jointed tangent hard spheres. A semiempirical prescription for the contact value of the depletion potential between two spheres immersed in a sea of rods and the high temperature approximation are used, yielding a prescription for the contact value of the sphere-sphere radial distribution function in hard-rod–hard-sphere mixture that depends on the needle density. When compared with the old formula [29] the new functional gives slightly broader phase coexistence envelopes but the changes affect mainly the polymer-rich binodal branches. In the long-chain limit the critical needle density tends toward a finite value almost independent on the size ratio q.

We have also analyzed the structure of hard-rod–polymer mixtures close to a hard wall. An increase of the chain length leads to an increase of the average polymer segment contact value. This behavior may lead to a qualitative difference of the polymer segment profiles, from an effective repulsion to an effective attraction, and to the opposite sign of the excess adsorption. By analyzing the orientational order parameter profiles we have found that the polymer coils decrease the tendency of needles to adopt anisotropic configurations.

It would be of interest to investigate interfacial behavior and in particular the wetting of the hard wall in such systems. One can expect a wealth of surface phase transitions, similar to that found in Ref. [24]. Another research direction is to take into account the rod-rod excluded volume interactions, similar in spirit to recent theory proposed by Esztermann and Schmidt [23]. This would open a possibility of the orientational phase transitions in such systems. Some of these topics are currently being investigated.

ACKNOWLEDGMENTS

We thank J. M. Brader for helpful suggestions regarding numerical implementation of the present theory. This work has been supported by KBN of Poland under Grant 3T09A 069 27.

[1] A. P. Gast, C. K. Hall, and W. B. Russell, J. Colloid Interface Sci. **96**, 251 (1983).
[2] S. Asakura and F. Oosawa, J. Chem. Phys. **22**, 1255 (1954).
[3] A. Vrij, Pure Appl. Chem. **48**, 471 (1976).
[4] R. Tuinier, J. Rieger, and C. G. de Kruif, Adv. Colloid Interface Sci. **103**, 1 (2003).
[5] D. G. A. L. Aarts, M. Schmidt, and H. N. W. Lekkerkerker, Science **304**, 847 (2004).
[6] J. M. Brader, R. Evans, M. Schmidt, and H. Löwen, J. Phys.: Condens. Matter **14**, L1 (2002).
[7] M. Dijkstra and R. van Roij, Phys. Rev. Lett. **89**, 208303 (2002).
[8] W. K. Wijting, N. A. M. Besseling, and M. A. Cohen Stuart, Phys. Rev. Lett. **90**, 196101 (2003).
[9] W. K. Wijting, N. A. M. Besseling, and M. A. Cohen Stuart, J. Phys. Chem. B **107**, 10565 (2003).
[10] G. H. Koenderink, G. A. Vliegenthart, S. G. J. M. Klujitmans, A. van Blaaderen, A. P. Philipse, and H. N. W. Lekkerkerker, Langmuir **15**, 4693 (1999).
[11] G. H. Koenderink, D. G. A. L. Aarts, V. W. A. de Villeneuve, A. P. Philipse, R. Tuinier, and H. N. W. Lekkerkerker, Biomacromolecules **4**, 129 (2003).
[12] L. Helden, R. Roth, G. H. Koenderink, P. Leiderer, and C. Bechinger, Phys. Rev. Lett. **90**, 048301 (2003).

[13] P. Bolhuis and D. Frenkel, J. Chem. Phys. **101**, 9869 (1994).
[14] R. Evans, in *Fundamentals of Inhomogeneous Fluids*, edited by D. Henderson (Marcel Dekker, New York, 1992), p. 85.
[15] Y. Rosenfeld, Phys. Rev. Lett. **63**, 980 (1989).
[16] Y. Rosenfeld, Phys. Rev. E **50**, R3318 (1994).
[17] A. Chamoux and A. Perera, J. Chem. Phys. **104**, 1493 (1996).
[18] A. Chamoux and A. Perera, J. Chem. Phys. **108**, 8172 (1998).
[19] S. Dubois and A. Perera, J. Chem. Phys. **116**, 6354 (2002).
[20] M. Schmidt, Phys. Rev. E **63**, 050201(R) (2001).
[21] P. Bolhuis, J. M. Brader, and M. Schmidt, J. Phys.: Condens. Matter **15**, S3421 (2003).
[22] J. M. Brader, A. Esztermann, and M. Schmidt, Phys. Rev. E **66**, 031401 (2002).
[23] A. Esztermann and M. Schmidt, Phys. Rev. E **70**, 022501 (2004).
[24] R. Roth, J. M. Brader, and M. Schmidt, Europhys. Lett. **63**, 549 (2003).
[25] R. Roth, R. van Roij, D. Andrienko, K. R. Mecke, and S. Dietrich, Phys. Rev. Lett. **89**, 088301 (2002).
[26] M. Schmidt and C. von Ferber, Phys. Rev. E **64**, 051115 (2001).
[27] J. M. Brader, C. von Ferber, and M. Schmidt, Mol. Phys. **101**, 2225 (2003).
[28] R. P. Sear, Phys. Rev. E **66**, 051401 (2002).
[29] P. Bryk, Phys. Rev. E **68**, 062501 (2003).
[30] Y.-X. Yu and J. Wu, J. Chem. Phys. **117**, 2368 (2002).
[31] M. S. Wertheim, J. Chem. Phys. **87**, 7323 (1987).
[32] R. Roth, R. Evans, A. Lang, and G. Kahl, J. Phys.: Condens. Matter **14**, 12063 (2002).
[33] Y.-X. Yu and J. Wu, J. Chem. Phys. **117**, 10156 (2002).
[34] Y. Rosenfeld, M. Schmidt, H. Löwen, and P. Tarazona, Phys. Rev. E **55**, 4245 (1997).
[35] P. Bryk, R. Roth, K. R. Mecke, and S. Dietrich, Phys. Rev. E **68**, 031602 (2003).
[36] R. Roth, J. Phys.: Condens. Matter **15**, S277 (2003).
[37] K. Yaman, C. Jeppesen, and C. M. Marques, Europhys. Lett. **42**, 221 (1998).
[38] P. Bolhuis, E. J. Meijer, and A. A. Louis, Phys. Rev. Lett. **90**, 068304 (2003).
[39] A. Yethiraj and C. K. Hall, J. Chem. Phys. **95**, 3749 (1991).
[40] E. Kierlik and M. L. Rosinberg, J. Chem. Phys. **100**, 1716 (1994).
[41] A. Yethiraj and C. K. Hall, Mol. Phys. **73**, 503 (1991).
[42] R. Hołyst, Mol. Phys. **68**, 391 (1989).